

The 671 nm Li I line in solar granulation

Dan Kiselman

The Royal Swedish Academy of Sciences, Stockholm Observatory, SE-133 36 SALTSJÖBADEN, Sweden

Received ; accepted

Abstract. The astrophysically very interesting Li I 671 nm line has been observed with high spatial resolution in solar granulation with the intention to diagnose departures from local thermodynamic equilibrium (LTE) in the line formation. The spectral feature is very weak, so this is also a test on the limits of such observations. The observations of the Li I line and other weak lines nearby are compared with the results of synthetic line calculations in three-dimensional granulation simulations. The dependence of line-centre velocities on photospheric continuum brightness is well described by the simulations. The observed equivalent width of the Li I line show an approximately flat dependence on continuum brightness, contrary to the theoretical LTE results. Detailed modelling of the line radiative transfer, with an approximate inclusion of three-dimensional effects, gives a better agreement with observations. The match is not perfect and various interesting reasons for this are considered. However, the possibility of systematic errors caused by the sensitivity of the Li I equivalent width to continuum placement calls for cautiousness in the conclusions.

1. Introduction

Stellar lithium abundances are the subject of many current debates in astrophysics (e.g., Thorburn 1996, Crane 1995, Spite & Pallavicini 1995). This paper continues the study of Li I line formation reported by Kiselman (1997), hereafter referred to as Paper I. The aim is to improve the understanding of lithium abundance determinations of solar-type stars by investigating the formation of lithium lines outside the classical realm of plane-parallel homogeneous photospheres and local thermodynamic equilibrium (LTE). It is also intended to test the idea put forward in Paper I that spatially resolved solar spectroscopy can be used to test NLTE results in less model-dependent ways than when just line profiles in integrated light are used. At the same time it tests the limits of such observational work since the lines studied are very weak.

Paper I was motivated by the proposal of Kurucz (1995) that lithium abundances derived for extremely metal-poor solar-type stars using 1D photospheric models and assuming LTE may be underestimated by as much as 1 dex due to 3D NLTE effects. The idea was that the transparency of “cold” regions in metal-poor photospheres would cause all lithium there to be ionised by ultraviolet radiation from “hot” regions. This would lead to a very weak line in the resulting mean spectrum, since the contribution to the spectral line from the hot regions is already small.

No such large effect of granulation on abundance determinations has yet been demonstrated by observations or detailed simulations. The standard behaviour of lines over the *solar* granulation pattern seems to be that lines – irrespective of the ionisation stage – get stronger in bright granules and weaker in darker intergranular lanes (Steffen 1989, Kiselman 1994). Thus one can expect that the influence on abundance ratios, which are derived from line ratios, will not be excessively large (Holweger et al. 1990).

The investigation of Li I line formation in a 3D model of solar granulation in Paper I demonstrated that the Kurucz mechanism at least does not work in solar granulation. This is also the conclusion of Uitenbroek (1998) who used a different NLTE treatment but the same kind of granulation model.

As regards metal-poor stars, the final verdict must of course wait until we know more about the inhomogeneity properties of their photospheres. This paper will only concern the solar Li I lines and is organised as follows. First the simulations are discussed in somewhat more detail than in Paper I. Then the solar observations are described, and finally the observations are compared with the simulation results.

2. Simulations

2.1. Principles

The availability of computing methods, atomic data, and powerful computers may just begin to allow realistic and consistent solutions of 3D NLTE problems in media such

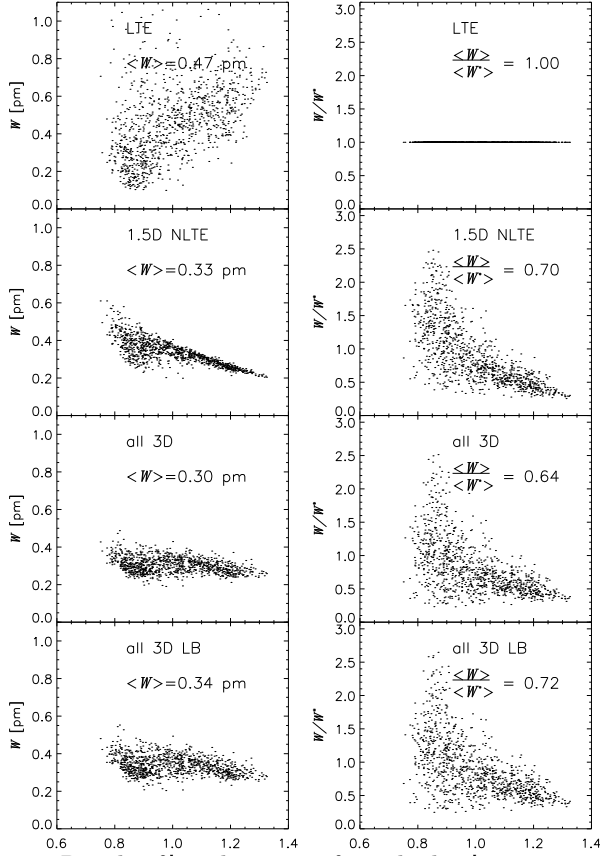


Fig. 1. Results from line transfer calculations in a granulation snapshot using different treatments and approximations: Li I equivalent widths as function of continuum intensity (left) and the ratio of these to the corresponding LTE values (right). Labels are explained in text. The mean values given are intensity-weighted means

as photospheric granulation – meaning large, and essentially complete, model atoms and full coupling between all angles. But such problems are still normally approached with some compromising with regard to atomic models, radiative transfer, or geometry. The aim of Paper I was mainly to study the effects of LTE departures and 3D effects on the Li I lines by comparing different spectral-line treatments in a single solar-granulation-model snapshot, with standard 1D models only used as a qualitative reference. The methods that were introduced, and are used also here, involve the calculation of line profiles and equivalent widths with a hybrid technique using a 1D NLTE code and a 3D background radiation field computed in LTE. This approach was chosen because it allowed a rather simple application of existing codes and because the very low solar lithium abundance makes it likely that the line radiative transfer problem can be treated as a continuum problem.

2.2. 3D photospheric models

The 3D photospheric models are two snapshots from the granulation simulations of Nordlund & Stein (e.g., Stein & Nordlund 1989, Nordlund & Stein 1991) that were also used by Kiselman & Nordlund (1995) – see that paper for illustrations. The snapshots are chosen so that they represent opposite phases in the (internally excited) oscillation that is present in the simulations. The original simulation data consisted of a $125 \times 125 \times 82$ grid of thermodynamic quantities. These were cut and resampled to a $64 \times 64 \times 55$ grid, corresponding to $6 \times 6 \times 1$ Mm on the solar surface. The plots of Fig. 1 only show results for every second x and y grid point, thus 1/4 of the vertical columns. The snapshots are periodic in the horizontal directions and this is used in the radiative transfer calculations.

2.3. LTE treatment of lines

Several weak lines observed in the region around the Li I 671 nm line are also included in the analysis for reference. The lines which were found in the VALD data base (Piskunov et al. 1995) or in the Kurucz (1995) line list were modelled in LTE with the routines of Kiselman & Nordlund (1995). The adopted line parameters are given in Table 1.

2.4. Non-LTE Li I line transfer calculations

The Li I line of interest is the resonance doublet at 671 nm which is very weak in the solar spectrum due to the low lithium abundance – the standard value $A_{\text{Li}} = \lg \frac{N(\text{Li})}{N(\text{H})} + 12 = 1.16$ (Grevesse et al. 1996; Müller et al. 1975) is used here. The doublet is blended with several other weaker lines all of which are not identified – see Braut & Müller (1975) and Kurucz (1995). The stronger (shorter wavelength) doublet component is less blended. The lines are also subject to hyperfine splitting and isotopic splitting that cause complications when modelling the line.

The Li I line profiles and equivalent widths were computed with version 2.2 of the plane-parallel NLTE code MULTI (Carlsson 1986) which uses the operator perturbation techniques of Scharmer & Carlsson (1985). All calculations of lines in emergent light were done for disk centre, i.e. for $\mu = 1.0$.

The 30-level lithium atomic model of Carlsson et al. (1994) was used with one change: the 671 nm resonance line was treated as a single line and not as a blended doublet. This was done because the current version of MULTI will not treat the radiative transfer correctly when the (microscopic) line profile is asymmetric in the presence of macroscopic velocity fields. This treatment of the doublet as a single line will not cause errors of importance for the current study since the line is very weak in almost all cases discussed here, putting it safely on the linear part of its curve of growth. This is confirmed by the fact that the

lithium abundance can be increased a factor of ten without changing the qualitative behaviour of the line. The change in line-formation height is apparently not significant for the NLTE behaviour. Thus the equivalent width of each line component will be proportional to the doublet equivalent width. The absolute solar Li abundance will not be a central issue here and line strengths will frequently be rescaled.

The option of providing MULTI with a background radiation field for calculation of the photoionisation rates was used in all calculations that are presented here and in some cases also for bound-bound transitions. The background radiation field was computed using routines written in the IDL data processing language that are similar to those used by Kiselman & Nordlund (1995). The equation of transfer was solved along a set of rays – five inclination angles ($\cos\theta = \mu$) and eight azimuthal angles (ϕ) – and the resulting intensities along each ray were used to calculate a mean intensity J_ν in each (x, y, z) point. This was done with a pure Planckian source function without any allowance for scattering (i.e. in what is sometimes called “strong LTE”). Some interpolation problems appeared close to $\tau_c = 1$ where the horizontal gradients are strong. This caused spurious values of J_ν in a few points but too deep down to have any impact on the resulting line profiles.

The hybrid treatment can make one worry about inconsistencies. It is important that the opacities used for production of the granulation model, the background radiation field, and the non-LTE calculations are compatible since a small difference may cause the optical surface to fall at different depths with large effects on the resulting outgoing intensities. Direct comparisons of the opacities showed that the differences were indeed insignificant within the context of the current study.

The presence of large amounts of spectral lines, especially in the blue and ultraviolet, is known to cause significant depression of the fluxes in these spectral regions. To somewhat allow for this, the OSMARCS plane-parallel LTE model-photosphere code (Edvardsson et al. 1993) was used to produce a solar model from which flux-weighted mean opacities were computed for a wavelength range around the wavelengths used in the computation of photoionising radiation fields. The ratio between these mean opacities, including spectral-line blocking, and the continuous opacities was then used to correct the opacities in the computation via interpolation in temperature. The correction factors range from 1.0 at high temperatures in the deep layers to well above 10 in the low-temperature regions.

2.5. Collisions with neutral hydrogen

The importance of inelastic collisions with neutral hydrogen atoms for photospheric line formation has been debated (e.g., Steenbock & Holweger 1984, Caccin et al. 1993, Lambert 1993). Such processes were not included

here. It could, however, be interesting to see if spatially resolved spectroscopy would offer a possibility to decide this issue and pin down the relevant cross sections. Tests where collisional rates were included according to the recipe of Steenbock & Holweger (1984) showed, however, that the changes introduced by the additional collisions were much too small in this case to allow any observational test.

2.6. Results

The left-hand plots of Fig. 1 shows the equivalent width W of the Li I 671 nm line as a function of continuum intensity I_c for one of the snapshots. Each point in the plots corresponds to one (x, y) column in the simulation snapshot. The plots in the right column show the departure from the LTE result in the form of W/W^* ratios, once again as a function of continuum intensities. From top to bottom, the plots show the results of line calculations with increasing sophistication. This series illustrates the importance of the departures from LTE caused by lateral photon exchange and the impact of ultraviolet line blanketing.

The uppermost pair of plots (**LTE**) shows the LTE result that was discussed in some detail in Paper I. Here the local temperature sets the line source function and the line opacity according to the Saha and Boltzmann equilibria. The result is that the line generally is strongest in the continuum-bright regions but the $I_c - W$ relation shows a significant scatter.

Leaving the LTE approximation gives the result in the second pair of plots (**1.5D NLTE**). Here the line strengths have been calculated in NLTE, so that each column of the snapshot is treated like a plane-parallel model with horizontal photon exchange neglected. The result is a narrow dependence of equivalent width on continuum intensity since now the atomic level populations are governed by a radiation temperature that is set in the lower regions where the continuum is formed. The experiments in Paper I showed that it is the bound-bound radiative transitions of Li I that matters, ultraviolet overionisation has little importance for the departures from LTE.

The third row (**all 3D**) shows the results when all lines have been calculated as fixed rates given by the 3D radiation field. Now the value of the mean intensity J_ν in each point is influenced by horizontally neighbouring regions and this gives a larger spread in the plot since the continuum intensity on the plot axis is the intensity coming from straight below.

The final modelling (**all 3D LB**) – which is to be compared with observations later – is represented by the lowest pair of plots in Fig. 1. Here all transitions are treated as fixed with the 3D radiation field and that field has been corrected for line blanketing as described above. The effect of the schematic line-blanketing correction is to increase the line strength somewhat due to the damping effect this has on the line-pumping-induced overionisation. The difference from the LTE plot is still significant and it seems

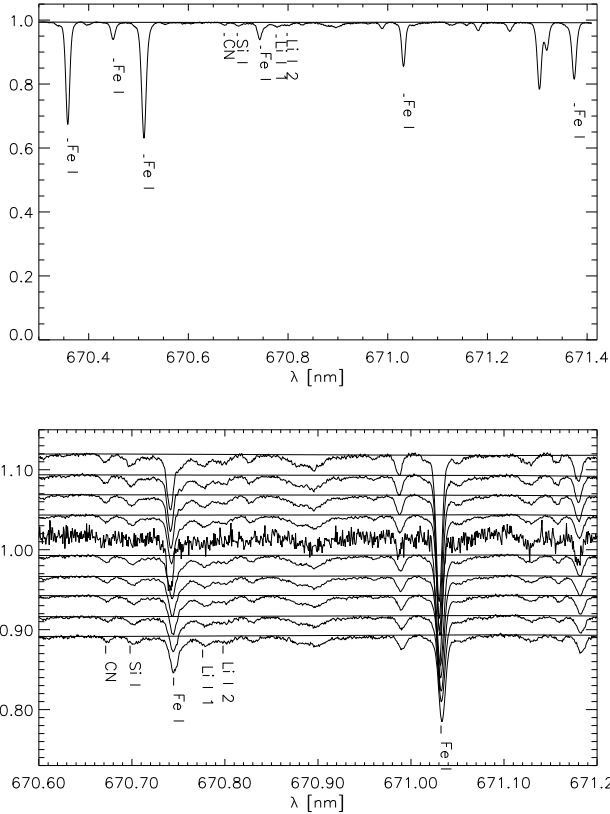


Fig. 2. The upper panel shows the mean spectrum from one exposure with the lines that are included in the study marked. The lower panel shows the binned spectra in the region around the Li I feature. One single unbinned spectrum is included for reference. Li I 1 marks the main doublet component which is the one that is measured. The continua that are fitted to the spectra are shown

possible to discern between the two cases observationally as will be tried in the next section.

Uitenbroek (1998) studied Li I line formation with a consistent 2D NLTE treatment, a similar granulation snapshot, but a smaller model atom than the one of this paper. The results are qualitatively similar to those presented here, but the discussion of them differs somewhat in that ultraviolet overionisation is considered to be an important mechanism contrary to what was argued in Paper I.

3. Solar observations

3.1. Methods

The weakness of the Li I feature in the solar spectrum makes observations and analysis at high spatial resolution challenging. Spectroscopic observations of the Li I resonance doublet at 671 nm in the Sun were made with the 0.48 m Swedish Vacuum Solar Telescope (SVST) on La Palma in October and November 1995. The Littrow spectrograph described by Scharmer et al. (1985) was used

Table 1. Adopted quantities for the spectral lines and the compilations from which they were taken

	λ [nm]	χ_l [eV]	g_l	g_u	f
Fe I	670.36	2.76	1	1	$6.90 - 4^a$
Fe I	670.45	4.22	1	1	$2.19 - 3^a$
Fe I	670.51	4.61	1	1	$3.19 - 2^a$
CN	670.67	2.76	46	46	$3.68 - 4^b$
Si I	670.70	5.95	1	1	$3.31 - 3^b$
Fe I	670.74	6.45	5	5	$5.89 - 2^b$
Li I	670.78	0.00	2	6	$7.53 - 1^d$
Fe I	671.03	1.49	1	1	$1.32 - 5^a$
Fe I	671.37	4.80	1	1	$2.51 - 2^a$

^a VALD data base (Piskunov et al. 1995)

^b Kurucz (1995)

^c Kurucz (1995), f multiplied with 1000

^d Carlsson et al. (1994)

The lines with $g_u = 1$ and $g_l = 1$ had only gf values available.

with an extra mask inserted in the spectrograph housing to block reflections from the Littrow lens. The spectrum was registered by a 10-bit Kodak Megaplug 1.6 CCD camera operating synchronously with a similar camera that imaged the slit-jaw. A spectrograph slit of $35 \mu\text{m}$ width was used, corresponding to $0''.3$. This gives a nominal spectral resolution of $R = \frac{\lambda}{\Delta\lambda} = 230000$. All observations discussed here were made of quiet photosphere at solar disk centre ($\mu = 1.0$) on November 2, 1997. The exposure time was 150 ms.

The first part of reductions were made with routines written for the purpose in the ANA interactive data processing language (Shine et al. 1988, Hurlburt et al. 1997).

Flat-fielding of the spectral frames is a problem since there is no continuous light source suitable to stand in for the Sun. The method introduced by Lites et al. (1990) employs the summing up of defocused exposures taken while the telescope scans over the solar disk. A mean spectrum is constructed for each frame by summing over the spatial direction. The resulting spectral frames are then divided with their mean spectra to get a flat field. The problem with this procedure is that unwanted systematic vertical structures cannot be removed and can even be created, e.g. by dust specks. To partially take care of this problem, a reference spectrum was made using several different grating settings so that each spectral region was recorded using different parts of the detector. Comparing the reference spectrum with the mean spectrum (from flat-field exposures) disclosed low-spatial-frequency variations which could then be corrected for. Apart from the flat-field and dark corrections, the spectra were corrected for geometrical distortions and put on a common intensity scale with the mean continuum intensity for an observational sequence as reference.

After all these treatments and corrections, close inspection of spectral frames, with the spectral lines and the continuum variations removed by division with a continuum mask and the mean spectrum, still showed a low-frequency fringe pattern with an amplitude of about 0.5%. This is the same order of magnitude as the relative depth of the lithium line. The fringes were removed by division with a sine-wave pattern whose parameters were found by a combination of least-square fitting and eye estimates. At the same time, the spectral frames were corrected to have the same choice of continuum level as that of Brault & Müller (1975).

The resulting spectra differ from the output of a perfect instrument due to image degradation by the atmosphere and the telescope, and scattered light in the spectrograph after the slit. The impact of the former may be assessed by measuring the continuum contrast in the spectra and looking at the simultaneous slit-jaw image, the importance of the latter can be deduced by comparing strong spectral lines with a solar atlas of high spectral resolution and purity. The strong Ca I line at 672 nm was observed to have a residual intensity of 0.41 of the continuum level compared to 0.35 in the digital issue of the solar atlas of Delbouille et al. (1973). If this difference is interpreted as the result of the addition of uniform stray light, the level of this stray light is about 10% of the “true” continuum level. This is apparently not unusual for single-pass instruments though it seems that to diagnose the origins of such straylight can be difficult (Gulliver et al. 1996).

Seventeen of the best spectra were chosen for further analysis (from now on using routines written in the IDL data processing language), they consist of 1523×879 arrays corresponding to $1.1 \text{ nm} \times 1'12''$. The pixelsizes in the spectral and the spatial direction oversamples the diffraction-limited spatial resolution ($\sim 0''.3$) and the nominal spectral resolution ($\sim 3 \text{ pm}$). The RMS intensity contrast of the spectra, as measured along the full length of the slit in a continuum spectral region, is around 6%. This is a quality measure on the spectra that shows that the current observations do not rival the best ever achieved with this instrument, probably those of Lites et al. (1989), but are still good.

It is not possible to examine the Li I feature in each spectral row since the S/N there is not high enough to allow reliable continuum determinations for such weak lines. Thus, the spectra were binned for each frame according to continuum intensity so that the variation of line properties with photospheric brightness may be investigated. For sufficiently strong and unblended lines, simple integration, without any assumption on line shape, is the best way to get equivalent widths. For the weakest lines, a Gaussian profile was fitted to the central part of the line feature. The equivalent width of the Li I feature measured in this way – the profile is fitted to the strongest and least blended doublet component – will not be equal to the true equivalent width for the whole doublet. But since the line is on

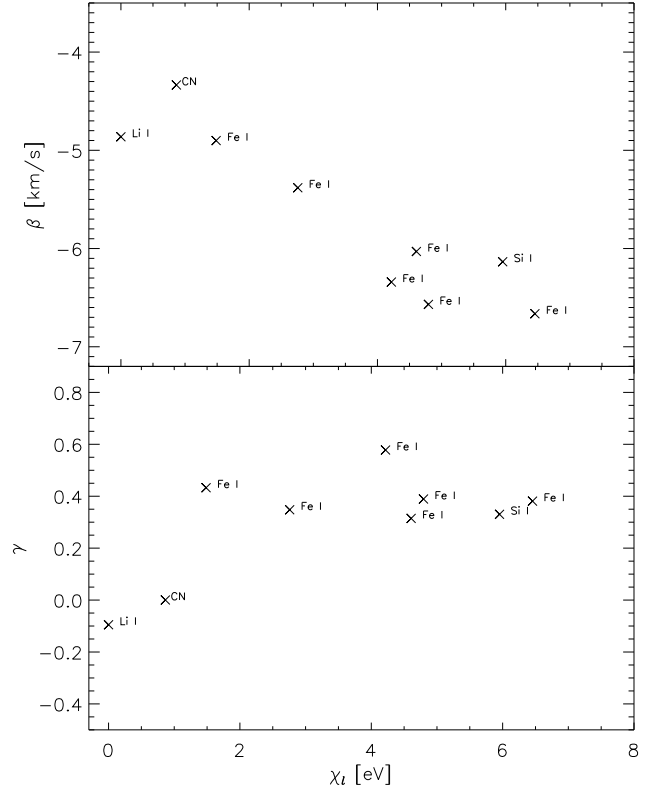


Fig. 5. Plots showing the sensitivity on continuum intensity of observed line parameters to the excitation energies of the lines’ lower levels. $\beta = \frac{dv}{dI_c} \cdot \langle I_c \rangle$, the slope of the line-centre velocities. $\gamma = \frac{dW}{dI_c} \cdot \frac{\langle I_c \rangle}{\langle W \rangle}$, the normalised slope of the equivalent widths.

the linear part of its curve of growth, the measured value will be closely proportional to the “real” equivalent width which corresponds to what we get from theory. Figure 2 shows the binned spectra for one frame together with one single spectral row.

In the further analysis of the data, the binned spectra with less than 20 single contributing spectra were discarded in order to decrease the noise. These represent the extremes of the continuum intensity range.

4. Comparison of observations with simulations

4.1. Smearing and binning of the simulations

In order to allow a fair comparison between simulations and observations, the simulated results must be treated in a way that mimics the effects of the atmosphere, the telescope, and the spectrograph. For this study, a simple model using the convolution with two Gaussians, one narrow and one wider with lower amplitude, was chosen. The FWHM:s and the relative amplitudes of the Gaussians

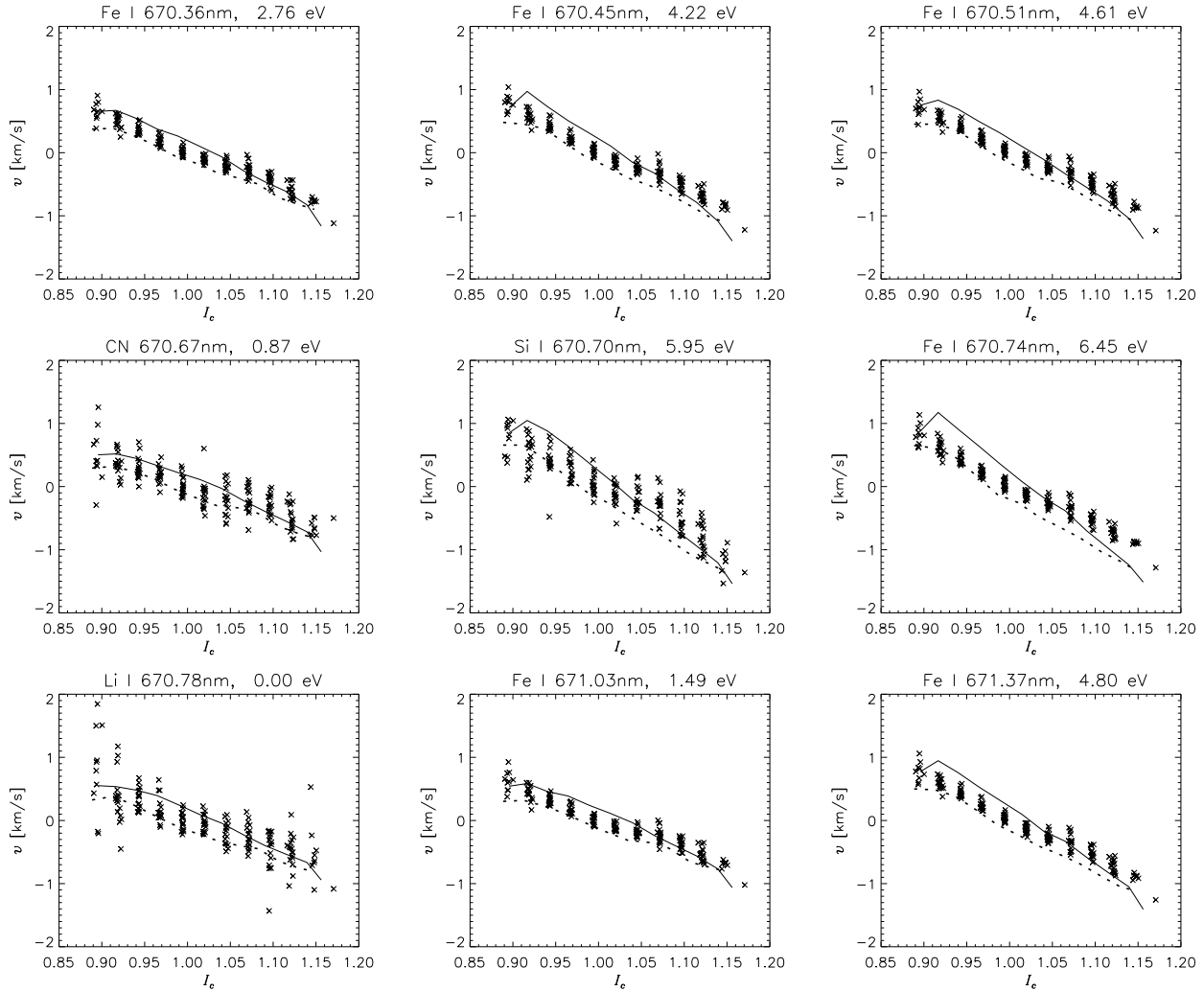


Fig. 3. Comparison of line-centre velocities v and their dependence on continuum intensity I_c as measured from binned observed spectra (crosses) with LTE simulations in two granulation snapshots (dashed and solid lines) for several weak spectral lines in the same spectral region as Li I

were chosen through experiments. The intensities, equivalent widths, and line-centre positions from the simulation were smoothed with various combinations of parameters until a combination was found that gave reasonable RMS-contrasts and the simulated intensity image looked similar to slit-jaw images. The FWHM of the narrow Gaussian corresponds to $0''.5$ and that of the broader curve, with an amplitude of 0.25 of the narrow one, to $4''.3$.

The experiments showed that the basic feature used here as a diagnostic, the $I_c - W$ diagram, did not change dramatically in shape when smoothed in different ways. Thus the detailed smoothing procedure used is not crucial to the results (though not unimportant).

Finally, the simulation results were binned in the same way as the observational spectra. Since the simulated data is noiseless, the lines that show simulation results in the figures represent the mean quantities for each bin.

4.2. Discussion

4.2.1. All lines

Figure 3 shows the observed and predicted line-centre velocities as function of continuum intensity, measured from binned spectra. The theoretical data come from the LTE simulations. A constant has been added to the velocities so that the intensity-weighted mean velocities for all data sets are zero. The correspondence is generally good, giving some confidence in the methods and models used here.

Figure 4 shows similar plots for equivalent widths. The theoretical values have been multiplied by a constant so that their intensity-weighted mean values coincide with that of the observations. The observed equivalent widths (binned) are well described by the simulations for some lines but not for others. The Fe I lines seem to be reasonably well described by the LTE modelling though with some deviations. The behaviour of the Si I line is well re-

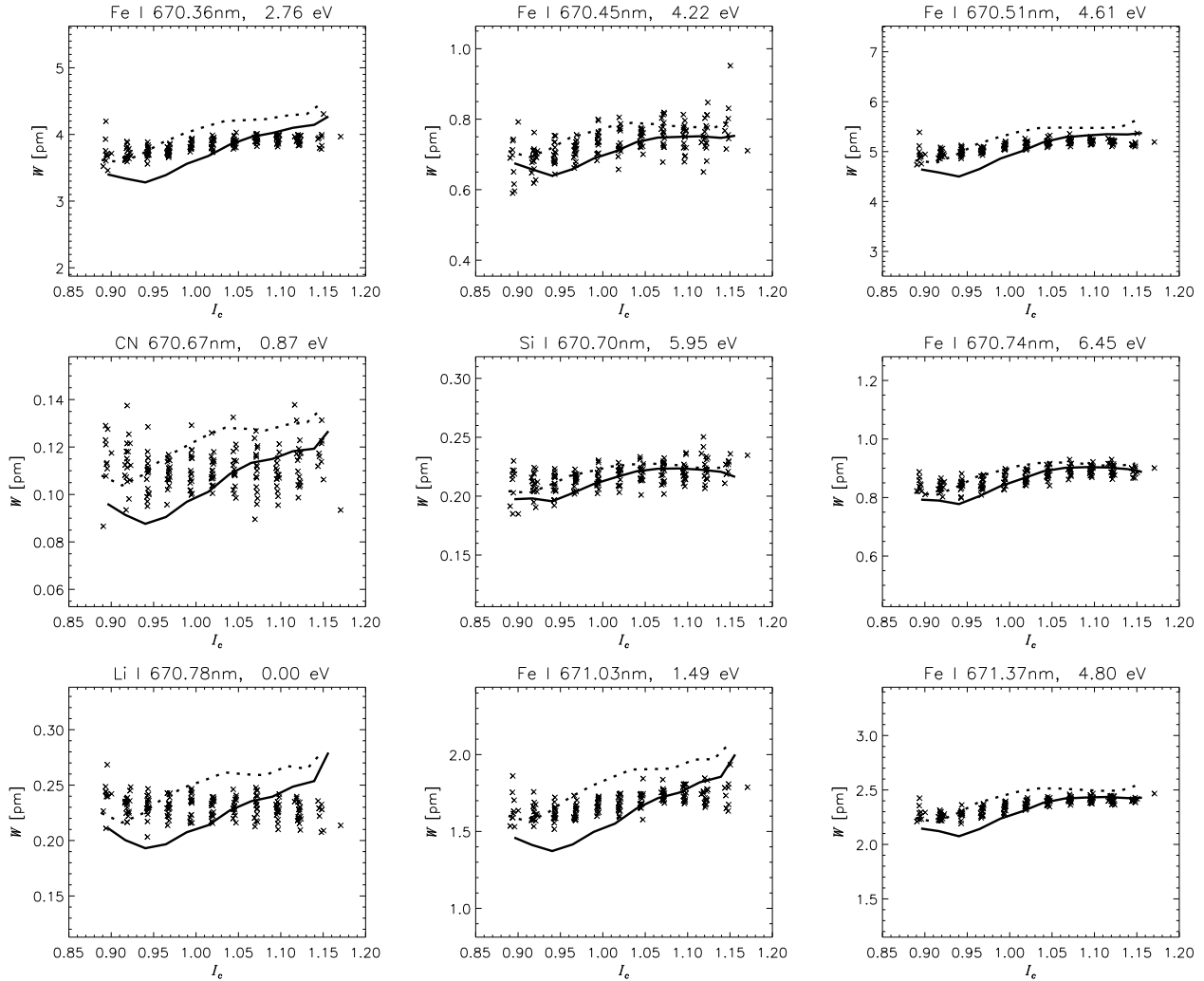


Fig. 4. Comparison of equivalent widths W measured from binned observations (crosses) with LTE simulations in two granulations snapshots (dashed and solid lines) for several weak spectral lines in the same spectral region as Li I

produced. The CN line shows what appears to be a discrepant behaviour, but the weakness of the line calls for cautiousness in the interpretation. The discrepancy between observations and LTE theory for the Li I seems more significant. The observed $I_c - W$ relation shows a weak slope in the opposite direction to the predicted LTE curves.

The central idea of this paper is that discrepancies between the theoretical LTE results and the observations of Fig. 4 are due to NLTE effects. Such conclusions are valid *if* we can trust the granulation models and the observational data. The following discussion will concentrate on the Li I line because of the (purported) reliability of the NLTE modelling for this light atom, which can be represented with an essentially complete atomic model. For heavier atoms like Fe I, the problem of assembling sufficiently complete and precise atomic data makes NLTE spectral-line modelling difficult and always questionable. The Li I line is thus a good test case in theory, but its weakness introduces observational uncertainties.

4.2.2. Excitation-potential dependence

The different slopes in the diagrams just discussed are highlighted in Fig. 5 where the normalised slopes from the observational data are plotted against the lower-level excitation energies of the respective lines. The normalised measures of the slopes are defined as $\beta = \frac{dW}{dI_c} \cdot \langle I_c \rangle$ for the line-centre velocities and $\gamma = \frac{dW}{dI_c} \cdot \frac{\langle I_c \rangle}{\langle W \rangle}$ for the equivalent widths. The derivatives come from second-degree polynomial fits to the observational points and their values at mean intensity are given.

The upper plot of Fig. 5 shows that the line-core velocity slopes correlate well with excitation potential. This is most easily understood as caused by the high-excitation lines being formed at greater depths (and temperatures) where the vertical velocities are greater than higher up.

The equivalent-width slopes plotted in the lower plot do not show a clear correlation with excitation potential. The Fe I lines show slopes that do not increase for high-

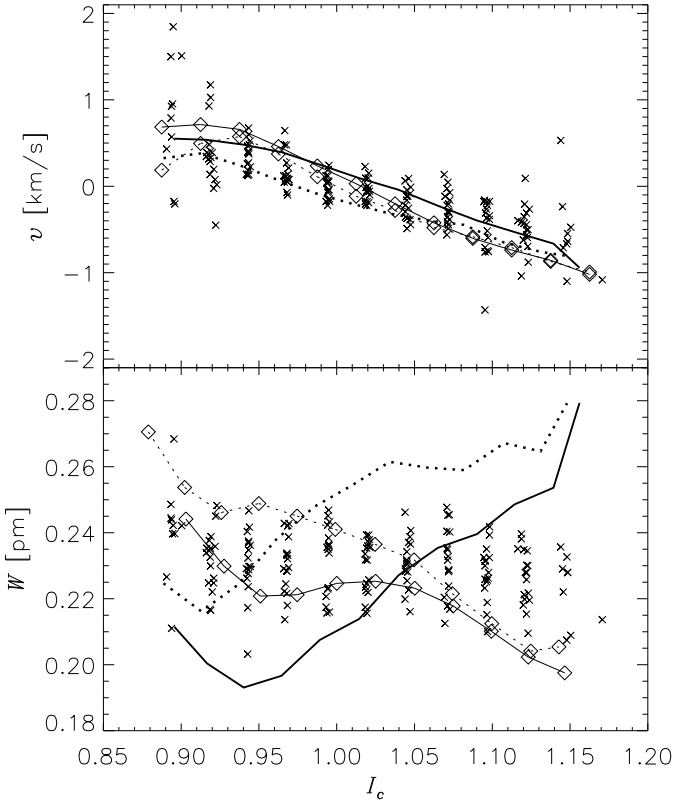


Fig. 6. Comparison of line-centre velocities (upper panel) and equivalent widths (lower panel) of the Li I 671 nm line measured from binned observational spectra (crosses) with LTE and NLTE simulations of the Li I 671 nm line. Each cross comes from one of seventeen exposures. Thick dotted and full-drawn lines are LTE simulations for the two granulations snapshots, lines with diamonds are NLTE. The theoretical values have been adjusted so that their mean values coincide with that of the observations

excitation lines. This is similar to what was found for the Fe I lines in Figure 5 of Kiselman (1994), and could be a manifestation of NLTE effects.

4.2.3. The Li I line

Figure 6 compares the observational line-centre-velocity and equivalent-width results for Li I with the theoretical predictions. The LTE results are the same as those in Figs. 3 and 4, the NLTE results are those labelled (**all 3D LB**) in Sect. 2.6 and Fig. 1.

The difference seen before between the theoretical LTE and NLTE equivalent-width results is now reduced because of the binning and smoothing operations. The spread among the observational points (crosses) at a specific intensity value is probably mostly due to random errors,

though there are also inherent differences from frame to frame. Note how this spread increases towards the limits of the plots due to fewer points from very bright or very dark regions contributing to each binned spectrum. (Remember that results from bins with fewer than 20 contributors are not shown.) In essence the observed equivalent widths fall in between the LTE and the NLTE curves, though closer to the latter. The NLTE curves fall inside the range of the observational points for most of the intensity range, but this is not the clear confirmation of the NLTE results one could have hoped for. The possible explanations for the discrepancy between observations and simulations can be summarised as follows.

The NLTE treatment. The discrepancy could be explained by underestimated collisional cross sections. This explanation would be the natural choice according to the central hypothesis of this paper. If we believe in the granulation models and the observational results, the most important (or uncertain) cross sections could in principle be determined by tuning them until there is correspondence between simulations and observations. The NLTE results are sensitive to the input J_ν values, which are computed in a simplified way with a coarse angular resolution. The discrepancy could be explained if J_ν in the visual region is underestimated in the dark regions relative to the bright ones. There is, however, no evident reason for this to be the case.

The granulation snapshots. While these kind of granulation simulations have demonstrated their realism, one must remember that many approximations have been employed in their computation – e.g. the finite spatial resolution that precludes the small structures which are certainly there in the real Sun. Possibly the two snapshots used are unrepresentative, but it should be noted that they are chosen to be independent and of opposite oscillatory phases. Also the apparent success in the LTE modelling (of both line strengths and line-centre velocities) for most of the other weak lines observed here is evidence for the snapshots being essentially realistic. Another piece of evidence for this is the general result that the (NLTE) Li I line strength depends more on the temperature structure at greater depths than on the kinetic temperature in the higher layers where the uncertainty of the granulation simulations can be expected to be greatest.

The smearing procedure. The smoothing of the simulations is made in a rather schematic way, but as discussed earlier, this is not likely to cause significant changes in the $I_c - W$ diagrams.

Blends. The Li I feature is contaminated by CN lines, as demonstrated by Brault & Müller (1975). According to their analysis, the contribution is relatively small. It should, however, make the measured $I_c - W$ dependence flatter according to the behaviour of the CN line in Fig. 4. If there is contamination of some other line, or if the CN contribution was much underestimated by Brault & Müller, this could explain the observed behaviour. This

would mean that the solar lithium abundance is significantly lower than previously thought. That would seem to be at odds with the behaviour of the Li I line in sunspots (e.g. Barrado y Navascués et al. 1996).

Systematic errors in the measured equivalent widths. These are difficult to estimate. A direct integration gives insignificant differences compared to the Gaussian profile fits, so the latter procedure is probably not a major source of error. In the same way, making the experiment of subtracting 10% of the mean light level from the spectral frames did not result in significant changes in the $I_c - W$ diagrams. Straylight is therefore not likely as an explanation for the discrepancy. The continuum placement is, however, crucial and expected to be the most important source of errors in the observational equivalent widths. An erroneously placed continuum will lead to an error in the $I_c - W$ slope that is not corrected when equivalent widths are rescaled with a constant factor. This was clear from the preliminary reduction work, though it should be noted that the algorithm for continuum fitting was chosen on what was considered to be objective grounds with the continuum level placed close to that of Brault & Müller (1975). The size of these errors is very difficult to estimate, but there is a clear possibility that they *could* be significant.

Were it not for the possibility of observational errors due to the continuum placement, the discussion would leave errors in the atomic data as the most probable explanation for the discrepancy. Problems with the granulation simulations, with the NLTE treatment or the possibility of blends would also be interesting to investigate further. The likely presence of systematic errors due to continuum-placement problems makes it, however, somewhat uncertain that the discrepancy is real and significant.

5. Conclusions

The observed $I_c - W$ relation for the Li I 671 nm line is rather flat and falls in between the theoretical LTE and the NLTE relations, though closer to the latter. It seems that the results exclude LTE as a line-formation hypothesis, something that is of interest in principle, though of course not very surprising. The NLTE modelling of this paper is at best only marginally confirmed, however. It is the extreme weakness of the Li I line that makes definite conclusions difficult to make. This is both because the necessary binning makes it impossible to study the spread in the $I_c - W$ plot and because the equivalent widths are sensitive to errors in the continuum placement. Spectra with better spatial resolution and/or higher S/N would probably allow firmer conclusions if they could be acquired.

The idea that spatially resolved spectroscopy may be helpful in revealing NLTE effects is still viable. It should be tested on somewhat stronger lines of other elements, even though their NLTE modelling is intrinsically more complicated and uncertain than for the relatively simple

Li I case. A coming paper (Kiselman, in preparation) will discuss similar solar observations and possible departures from LTE of a large set of Fe lines of different strengths.

Acknowledgements. I thank all staff of the SVST for assistance during the observations, Göran Scharmer also for comments on the manuscript, Martin Asplund and Rob Rutten are thanked for discussions, and Åke Nordlund for help with the granulation models.

References

- Barrado y Navascués D., De Castro E., García Lopez R.J., Sánchez Almeida J., Montesinos B., 1996, Li, Na, K and H α in a sunspot. In: Strassmeier K.G. (ed.), Poster Proc. IAU Symp. 176, Stellar Surface Structure. Institut für Astronomie der Universität Wien, p. 123
- Brault J.W., Müller E., 1975, Solar Phys. 41, 43
- Caccin B., Gomez M.T., Severino G., 1993, A&A 276, 219
- Carlsson M., 1986, Uppsala Astronomical Report No. 33
- Crane P. (ed.), 1995, The light element abundances. Springer, Berlin
- Carlsson M., Rutten R.J., Bruls, J.H.M.J. Shchukina N.G., 1994, A&A, 288, 860
- Delbouille L., Roland G., Neven L., 1973, Atlas photométrique du spectre solaire de λ 3000 à λ 10000. Université de Liège, Liège
- Edvardsson B., Andersen J., Gustafsson B., Lambert D.L., Nissen P.E., Tomkin J., 1993, A&A, 275, 101
- Grevesse N., Noels A., Sauval A.J., 1996, Standard abundances. In: Holt S.S., Sonneborn G., Cosmic abundances, Vol. 99, ASP Conference Series, p.117
- Gulliver A.F., Hill G., Adelman S.J., 1996, A spectrograph's instrumental profile and scattered light. In: Model atmospheres and spectrum synthesis, ASP Conference Series, Vol. 108, p.232
- Holweger H., Heise C., Kock M., 1990, A&A, 237, 510
- Hurlburt N., Shine R., Tarbell T., 1997, SPIE Proc., 3017, 165
- Kiselman D., 1994, A&AS, 104, 23
- Kiselman D., 1997, ApJ, 489, L107 (Paper I)
- Kiselman D., Nordlund Å., 1995, A&A, 302, 578
- Kurucz R.L., 1995, ApJ, 452, 102
- Lambert D.L., 1993, Physica Scripta, T47, 186
- Lites B.W., Nordlund Å., Scharmer G.B., 1989, Constraints imposed by very high resolution spectra and images on theoretical simulations of granular convection. In: Rutten R.J., Severino G. (eds.) Solar and Stellar Granulation. Kluwer Academic Publishers, p. 349
- Lites B.W., Skumanich A., Scharmer G.B., 1990, A&A, 355, 329
- Müller E., Peytremann E., de la Reza M., 1975, Solar Phys., 41, 43
- Nordlund Å., Dravins D., 1990, A&A, 228, 155
- Nordlund Å., Stein R.F., 1991, Granulation: non-adiabatic patterns and shocks. In: Gough, D.O. and Toomre, J. (eds.) Challenges to Theories of the Structures of Moderate Mass Stars. Springer, Heidelberg, p.141
- Piskunov N.E., Kupka F., Ryabchikova T.A., Weiss W.W., Jeffery C.S., 1995, A&AS, 112, 525
- Scharmer G.B., Brown D.S., Petterson L., Rehn J., 1985 Applied Optics, 24, 2558

- Scharmer G.B., Carlsson M., 1985, *J.Comput.Phys.*, 59, 56
- Shine R.A., Porter L.Z., Frank Z., Gurman J.B., Pothier D.,
Ferguson S., 1988, *A users guide to ANA*
- Spite F., Pallavicini R. (eds.), 1995, *Mem. Soc. Astron. Ital.*,
66
- Steenbock W., Holweger H., 1984, *A&A*, 130, 319
- Steffen M., 1989, Spectroscopic properties of solar granulation
obtained from 2-D numerical simulations. In: Strassmeier
K.G. (ed.), *Poster Proc. IAU Symp. 176, Stellar Surface
Structure. Institut für Astronomie der Universität Wien*,
p. 425
- Stein R. F., Nordlund Å., 1989, *ApJ*, 342, L95
- Thorburn J., 1996, Lithium in stars. In: Holt S.S., Sonneborn
G., *Cosmic abundances, Vol. 99, ASP Conference Series*,
p.165
- Uitenbroek H., 1998, *ApJ*, in press